

Analyst

Accepted Manuscript



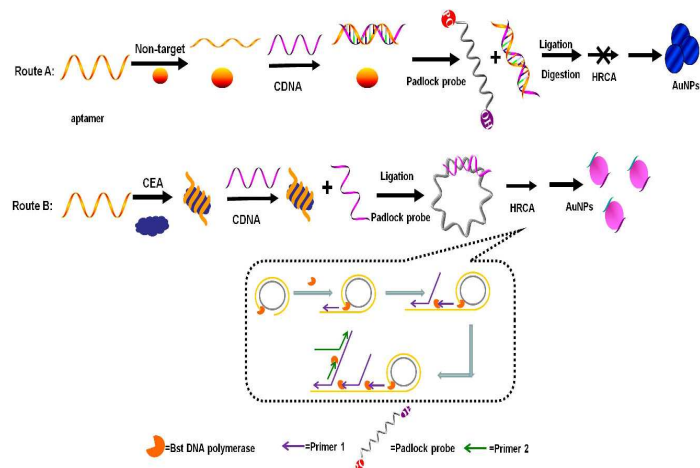
This is an *Accepted Manuscript*, which has been through the Royal Society of Chemistry peer review process and has been accepted for publication.

Accepted Manuscripts are published online shortly after acceptance, before technical editing, formatting and proof reading. Using this free service, authors can make their results available to the community, in citable form, before we publish the edited article. We will replace this *Accepted Manuscript* with the edited and formatted *Advance Article* as soon as it is available.

You can find more information about *Accepted Manuscripts* in the [Information for Authors](#).

Please note that technical editing may introduce minor changes to the text and/or graphics, which may alter content. The journal's standard [Terms & Conditions](#) and the [Ethical guidelines](#) still apply. In no event shall the Royal Society of Chemistry be held responsible for any errors or omissions in this *Accepted Manuscript* or any consequences arising from the use of any information it contains.

Table of content



5

A hyperbranched rolling circle amplification (HRCA) based colorimetric biosensor for carcinoembryonic antigen (CEA) with high sensitivity and specificity has been developed

1
2
3
4 A hyperbranched rolling circle amplification (HRCA) based colorimetric biosensor
5 for carcinoembryonic antigen (CEA) with high sensitivity and specificity has been
6 developed.
7
8
9
10
11
12
13
14
15
16
17
18
19
20
21
22
23
24
25
26
27
28
29
30
31
32
33
34
35
36
37
38
39
40
41
42
43
44
45
46
47
48
49
50
51
52
53
54
55
56
57
58
59
60

Cite this: DOI: 10.1039/c0xx00000x

www.rsc.org/xxxxxx

ARTICLE TYPE

Ultrasensitive Colorimetric Carcinoembryonic Antigen biosensor Based on Hyperbranched Rolling Circle Amplification

Kai Liang,^a Shui-ting Zhai,^a Zhi-dong Zhang,^a Xiao-yang Fu,^a Jing-wei Shao,^{b*} Zhen-yu Lin,^b Bin Qiu^{b*} and Guo-nan Chen^b

Received (in XXX, XXX) Xth XXXXXXXXXX 20XX, Accepted Xth XXXXXXXXXX 20XX

DOI: 10.1039/b000000x

In this study, a hyperbranched rolling circle amplification (HRCA) based colorimetric biosensor for carcinoembryonic antigen (CEA) has been developed with high sensitivity and specificity. CEA aptamer can bind with its target (CEA) to form a complex due to their high affinity. And the introduction of CDNA could not hybridize with the aptamer. Thus, the free CDNA can propagate HRCA reaction to form a large number of single-stranded DNA (ss-DNA). ss-DNA can be easily adsorbed onto AuNPs and prevent salt-induced AuNPs aggregation, which cause the changing of the color of the system. It is found that the absorbance intensity ratio (A_{520}/A_{660}) has a linear relationship with the concentration of target in the range of 5pM–0.5nM, and the detection limit is as low as 2pM. (S/N=3).

1. Introduction

Recent developments in biotechnologies offer a wide variety of signal amplification tools, such as polymerase chain reaction (PCR) and rolling circle amplification (RCA). Since PCR required complex thermal cycling steps, need sophisticated and expensive equipments, it is considered to be complicated. The process of RCA is much simple than that of PCR, which contains the following process: a short DNA primer (CDNA) hybridizes with the DNA template (padlock probe) to fold into a ringlike structure in a head-to-tail manner firstly. Then with the assistance of DNA ligase, the padlock probe is circularized, and the subsequent RCA process is accomplished by Phi 29 DNA polymerase.¹ But RCA the sensitivities of RCA-based biosensors are poorer than that of PCR.² In order to solve this problem, hyperbranched rolling circle amplification (HRCA) has been developed based on the RCA reaction,³ which is an isothermal and exponential amplification through turn-by-turn cascade of primer extension and strand displacement.^{4,5} The products of HRCA consist of large amounts of single-stranded DNA (ss-DNA) and double-stranded DNA (ds-DNA) with various lengths. Many HRCA based biosensor had been developed for high sensitivity detection.^{6,7} Mostly of these sensors are based on fluorescent or electrochemical detection, these approaches need complex labelling and usually require expensive measurement.

Au nanoparticles (AuNPs) represent a class of materials with a high extinction coefficient and a broad absorption in the visible range.⁸ Au atoms on the surface possess unoccupied orbital, which facilitate nucleophiles to donate electrons.^{9,10} It has been reported that ss-DNA and ds-DNA own different binding properties toward unmodified AuNPs.^{11,12} Because ss-DNA is flexible and can partially uncoil its bases, which can be easily

adsorbed onto AuNPs and prevent salt-induced AuNPs aggregation by enhancing the electrostatic repulsion between ss-DNA-adsorbed AuNPs, which results in the color changing of the solution. Many colorimetric assays had been developed based on this mechanism. For examples, Chang's group pioneered a colorimetric sensing approach for the determination of adenosine triphosphate using aptamer-modified gold nanoparticles.¹³ Luo et al. had developed a novel aptamer-based colorimetric biosensor for multiplex detection of adenosine, thrombin and cocaine.¹⁴ These studies demonstrated that colorimetric assays own the characters of simple, speedy and direct visual detection without the need for any complicated equipment,¹⁵ but the sensitivity is not well, this limits their application. It is necessary to find out some methods to improve the sensitivity of the colorimetric assay.

Ultrasensitive determination of disease-marker proteins have attracted substantial research efforts due to their broad applications in disease diagnosis, prevention, and treatment.¹⁶⁻¹⁸ Here, a highly sensitive and label-free method for analyzing protein on the basis of AuNPs-mediated HRCA had been developed. Carcinoembryonic antigen (CEA), one of the most studied tumor markers associated with liver, colon, breast and colorectal cancer, exists in endoblast origin digestive system cancer,¹⁹ had been chosen as a example. The assay is easy to implement for visual detection, which combines the merits of high sensitivity of HRCA and simple of Au-NPs based colorimetric sensor.

2. Experimental section

2.1 Chemicals

The sequence of CEA aptamer^{20,21} and the other DNA oligonucleotides were synthesized by Sangon Inc. (Shanghai,

China). Their sequences are shown below:

CEA aptamer: 5'-ATACCAGCTTATTCAATT-3'

CDNA: 5'-AATTGAATAAGCTGGTAT-3'

Primer 1: 5'-GCA TTT CAG TTT ACG-3'

Primer 2: 5'-TTG CGA AAT GTA AAC-3'

Padlock: 5'-P-TATTCAATT GCA TTT CAG TTT ACG GTT TAC ATT TCG CAA ATACGTGCT-3'

In the padlock probe, the binding region for the HRCA primer 1 was shown in wavy line, and the region with the same sequence as the HRCA primer 2 was shown in underlined portions. *Escherichia coli* (*E.coli*) DNA ligase set (including *Escherichia coli* DNA ligase, 10×*Escherichia coli* DNA ligase buffer, and 10×BSA (0.05%)) were obtained from Takara Biotechnology Co., Ltd. (Dalian, China). The deoxynucleotide solution mixture (dNTPs), Bst DNA polymerase large fragment, and their corresponding buffer were purchased from New England Biolabs (NEB). SYBR Green II was purchased from Xiamen Biovision Biotechnology Co. Ltd. (Xiamen, China). HAuCl₄(99.999%) and sodium citrate dehydrate were purchased from Dingguo Biotech (Beijing, China). All other chemicals were of analytical reagent grade and obtained from Sigma Chemical Co., USA. In this experiment, double distilled water (Milli-Q, Millipore, resistance 18.2-MΩ) was used throughout the experiments. DNA buffer solutions were prepared by dissolving DNA into 50 mmol/L Tris-HCl (pH 7.4).

2.2 HRCA reaction and AuNPs-based colorimetric assay

Different concentrations of CEA were mixed with aptamer probe (5 nM) by equal volume for 30 min. Then, the same volume of CDNA (5 nM) was introduced into above solution for incubation at 37 °C for 30 min with the vibration. The ligation reaction was performed in the ligation buffer solution containing 6 U *E. coli* DNA ligase, 0.05% BSA and 0.167mM nicotinamide adenosine dinucleotides (NAD), which was incubated at 37 °C for 60 min. And then, the HRCA reaction was carried out at 63 °C for 60 min simultaneously in above solution, which including 40 nM primer 1, 40nM primer 2, 9.6 U Bst DNA polymerase and 0.6 mM dNTP.

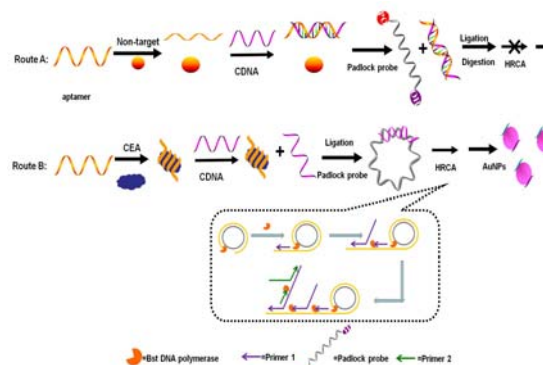
AuNPs with an average diameter of 13 nm were prepared according to the literature²². For the colorimetric assay, 50μL of HRCA product was added to 150 μL of the gold colloid and after mixing for some minutes, additional 15μL 3 M NaCl was added. Then the resulted solutions can be observed by naked eye or quantified by UV-Vis absorption spectra (Perkin Elmer Instruments, USA). Due to the difference between the aggregation degree of Au-NPs between absorbance at wavelength 520 nm and 660 nm, the ratio of Absorbance 520/Absorbance 660 (A520/A660) were chosen to examine the effect of proposed method.

3. Results and Discussion

3.1 Principle of the colorimetric biosensor

The protocol of the proposed colorimetric biosensor is shown in Scheme 1. In the absence of target (CEA), the aptamer can hybridize with CDNA to form ds-DNA and no CDNA hybridize with padlock to initiate the HRCA. Only padlock probe and HRCA primers exist in the solution and the dosage of primers cannot prevent salt-induced AuNP aggregation and the color of

the solution was blue (Route A). In the presence of target CEA, the CEA binding aptamer preferred to form CEA/aptamer complex in lieu of aptamer-CDNA duplex. Thus, the free CDNA can hybridize with the padlock probe in bold, which can be ligated and circularized in the presence of *E.coli* DNA ligase. The obtained circular padlock probes are further purified by digestion of the unreacted linear padlock probes and the excess oligonucleotides using Exonucleases I and III. Subsequently, the primer extension and strand displacement will take place in the presence of circular padlock probes, two primers, and Bst DNA polymerase, producing a large number of ss-DNA fragments in variable length. By this means, each target can propagate a HRCA reaction to form a large number of ss-DNA. Since ss-DNA can be easily adsorbed onto AuNPs and prevent salt-induced AuNPs aggregation, so the color of the solution is red (Route B). Based on this principle, a colorimetric method for CEA determination can be developed.



Scheme 1 Principle of the proposed HRCA based colorimetric biosensor

A simple experiment has been performed to verify our presumption. Firstly, faradic electrochemical impedance spectroscopy had been applied to characterize the binding between the aptamer and the targets(CEA). As shown in Fig.1(A), when the probe aptamer is immobilized on the gold electrode surface, the *R_{ct}* value is about 200.0 Ω (curve a) because the negative charged phosphate backbone on the electrode prevents the redox of [Fe(CN)₆]^{3-/4-} on the electrode. After treating with the target, the *R_{ct}* value shoots up to 544.9 Ω (curve b). The reason lies in that the aptamer/CEA was formed on the electrode, which retards the interfacial electron transfer reaction of the redox probe further. This result indicates that the aptamer can bind with CEA.

Since ss-DNA can combine with SYBR Green II to produce strong fluorescent signal, which has been applied to check the products of HRCA solution contains large amount of ss-DNA or not. As shown in Fig.1 (B), in the present of target CEA, an obvious fluorescent signal can be detected (curve a), indicating that the exist of target can trigger the HRCA reaction, which form a large number of ss-DNA. But in the absence of target, the fluorescent intensity is weak (curve b). The reason maybe lie in that nothing can trigger the HRCA reaction, a few of non-reaction primers combine with SYBR Green II to produce weak fluorescent signal. The HRCA products at different target concentrations are analyzed by gel electrophoresis experiments. As shown in the inset figure of Fig.1(B), longer ladder-type bands are observed in the

presence of 8×10^{-9} mol/L CEA (lane 1) and darker ladder-type band is observed in the presence of 8×10^{-10} mol/L CEA (lane 2). but no bands in the absence of CEA are observed (lane 0) because no HRCA occurs. These results suggesting the validity of the proposed mechanism.

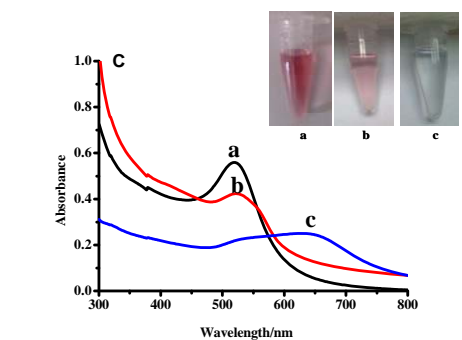
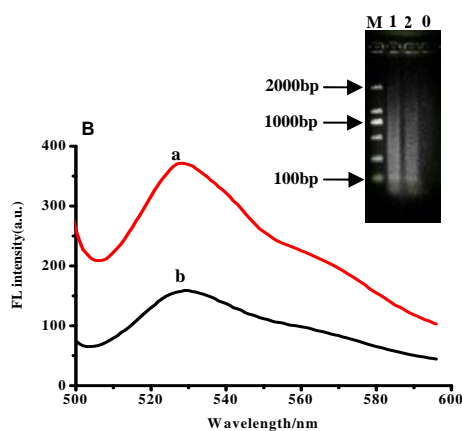
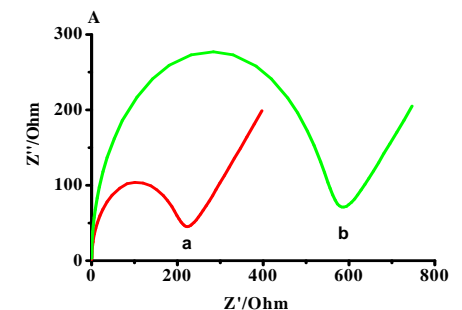
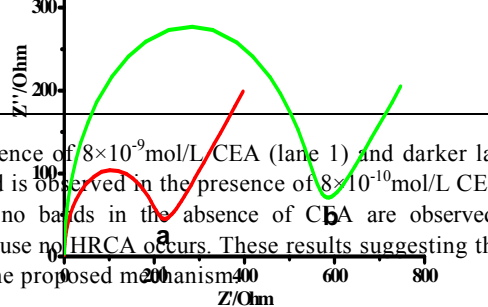


Fig. 1 (A) Nyquist plots of electrodes. a: probe aptamer /MCH modified gold electrode; b: aptamer /MCH modified gold electrode after interaction with 8×10^{-9} mol/L CEA. (B) Fluorescence spectra of HRCA solution with (a) and without (b) CEA ($[CEA]=8 \times 10^{-9}$ mol/L); Inset: HRCA products are electrophoresed in a 2% agarose gel. The DNA ladder is indicated in lane M. Lanes 0, 1, 2 represent the HRCA products from $[CEA]=0$, $[CEA]=8 \times 10^{-9}$ mol/L and $[CEA]=8 \times 10^{-10}$ mol/L, respectively. (C) UV-vis absorption of citrate-AuNPs (a), HRCA-AuNPs solution with (b) and without (c) CEA ($[CEA]=8 \times 10^{-9}$ mol/L)

Fig.1(C) shows the UV-vis absorption spectra and the corresponding photographs of AuNP colloids at different conditions. The color of citrate-AuNPs solution was red and the

absorption band was at around 520 nm (tube a and curve a in Fig. 1(C)). In the presence of CEA, the HRCA reaction can be initiated, and the color of AuNPs solution containing HRCA product after salt adjusting is red and the absorbance does not cause significant variation (tube b and curve b in Fig. 1(C)). But in the absence of target (CEA), nothing can trigger the HRCA reaction. Only HRCA primers exist in the solution, and the dosage of primers cannot prevent salt-induced AuNPs aggregation. At this stage, the color of the AuNPs solution containing HRCA primers after salt adjusting is blue and a new absorption band at around 660 nm appeared and the intensity at around 520 nm decreased (tube c and curve c in Fig. 1(C)). These results also demonstrate the feasibility of the proposed system.

3.2 Optimized of the reaction conditions

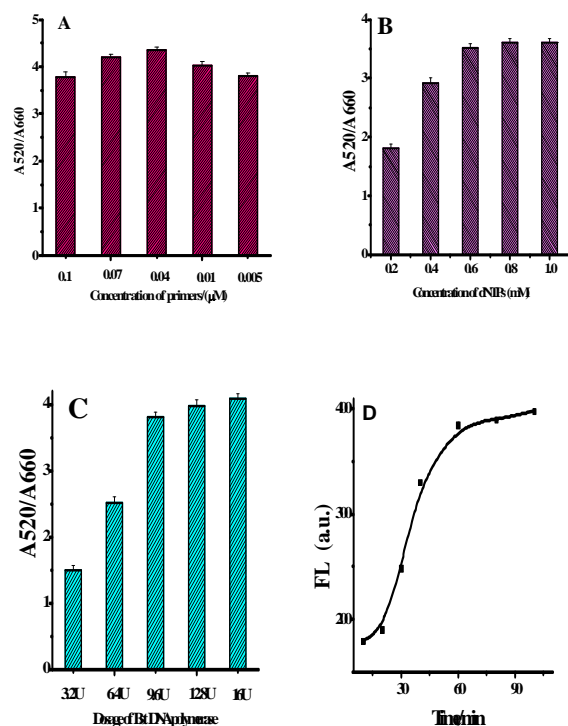


Fig. 2 The effects of the concentrations of (A) primers, (B) dNTP and (C) Bst DNA polymerase on the absorbance intensity ratio in the presence of 8×10^{-9} mol/L CEA. (D) SYBR GREEN II based time-dependent fluorescence intensity changes in HRCA reaction ($[CEA]=8 \times 10^{-9}$ mol/L)

To obtain high amplification efficiency of HRCA, the concentrations of primers, dNTP substrates and Bst DNA polymerase are optimized. As shown in Fig. 2(A), the absorbance intensity ratio (A_{520}/A_{660}) increased with the increasing of primers concentration from 0.005 μ M to 0.04 μ M, suggesting that primer concentration leads to the improvement of HRCA efficiency. But when the concentration of primers exceeds 0.04 μ M, the absorbance intensity ratio (A_{520}/A_{660}) decreases. This can be explained by the fact that high concentration exogenous primers might adversely cause primer dimerization.²³ Therefore, 0.04 μ M is selected as the optimum concentration of primers in the

subsequent research. In addition, with the increment of dNTP concentration, A_{520}/A_{660} enhances gradually, and finally reaches a constant after 0.6 mM. Thus, the concentration of dNTP is 0.6 mM (Fig.2(B)). For the concentration of Bst DNA polymerase, it is found that A_{520}/A_{660} increased with the increasing of Bst DNA polymerase concentrations firstly and then reached a stabilized platform when the concentrations are bigger than 9.6 U (shown in Fig.2(C)). Hence, the concentration of Bst DNA polymerase is set as 9.6 U.

A long HRCA reaction time is expected to generate more copies of the products for better signal amplification. The SYBR GREEN II based time-dependent fluorescence has been applied to monitor the HRCA reaction. As shown in Fig.2(D), the fluorescent intensity boosts up gradually at the beginning, showing that the HRCA production is generated continuously. While the fluorescent intensity trends to a constant value at 60 min, indicating the saturation of HRCA production. Therefore, 60 min is chosen as the optimum time for HRCA reaction.

3.3 Quantitative analysis of CEA

To further characterize the detection range of this assay, a series of samples containing different concentrations of CEA have been tested. As shown in Fig.3(A), the color of the solutions changed gradually from red to blue upon the decreasing of the CEA concentrations. Meanwhile, a dramatic red shift can be observed with the decreasing of target concentration from the absorbance spectra of the detection samples. Only one peak located at 520 nm was detected in the presence of high concentration of CEA, along with the decreasing of the CEA concentration, a new broad absorption appeared, while the absorbance at 520 nm gradually red shifted and decreased. Accordingly, the absorbance peak ratio at 660 and 520 nm was employed to quantitatively scale the CEA concentration. A_{520}/A_{660} had a good linear relationship with the logarithmic concentration of CEA in the range of 5.0pM–0.5nM (Fig. 3(B)), and the regression equation can be expressed as:

$$A_{520}/A_{660} = 1.19 \log C + 14.57, R = 0.9946$$

where C is the CEA concentration and R is the correlation coefficient. A detection limit of 2.0 pM ($S/N=3$) was achieved, which is much lower than the early reported fluorescence²⁴, chemiluminescence²⁵ or electrochemical approaches²⁶. The reason may lie in the combination of high efficiency of HRCA and high specificity of aptamer.

Six replicated experiments had been performed at the CEA concentration of 50 pM, the relative standard deviation (RSD) was 5.8%, this means the proposed method has good reproducibility.

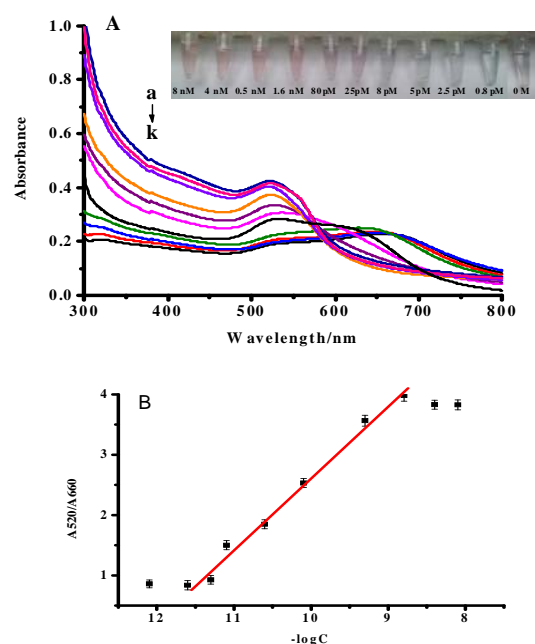


Fig. 3 (A) Color change of the solution with increasing concentrations of CEA and UV-vis absorption spectra of the system at different CEA concentration. From a to k: 8.0×10^{-9} ; 4.0×10^{-9} ; 1.6×10^{-9} ; 5.0×10^{-10} ; 8.0×10^{-11} ; 2.5×10^{-11} ; 8.0×10^{-12} ; 5.0×10^{-12} ; 2.5×10^{-12} ; 0.8×10^{-12} ; 0 mol/L. (B) The variation of absorbance intensity ratio against the different concentrations of CEA. Inset: the corresponding calibration plot of the logarithm of target CEA concentrations in the range from 5.0pM–0.5nM.

3.4 The specificity of HRCA based colorimetric assay

To demonstrate the specificity of the sensors for biological samples, several common proteins were used to test the selectivity of the proposed colorimetric sensor. 1 μ M alpha fetoprotein (AFP), lysozyme, bovine serum albumin (BSA) and thrombin were chosen as interferents and the concentration of CEA is set as 80 pM. From the visual observation (Fig. 4, inset), the color of the mixed solution still remain red only in the presence of CEA, resulting from the product of HRCA reaction prevent salt-induced AuNPs aggregation. When the concentrations of interferents were more than 10000 times higher than CEA concentration, the color of the salt-induced AuNPs solutions turn to blue and almost similar to the blank. The values of the absorption ratio (A_{520}/A_{660}) for the system treated with different target were also recorded (Fig. 5A) In the presence of 80pM CEA, the value increased much compared with the blank. While in the presence of 1 μ M other protein, the values were similar to or just a little higher than the value of the blank. The reason may lie in that no enough ss-DNA had been produced and induced the aggregation of AuNPs. This demonstrates that the HRCA-based biosensor is highly specific and has a good selectivity for discrimination of CEA from other proteins.

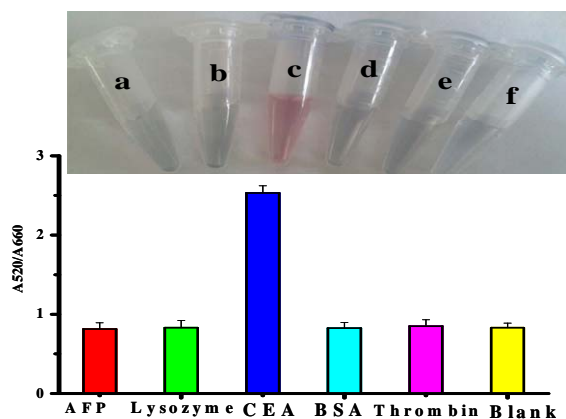


Fig. 4 The absorbance intensity ratio of the proposed sensor at different interferents and target. The inset is the corresponding color at different interferents and target. a: thrombin; b: AFP; c: CEA; d: BSA; e: lysozyme; f: blank. The concentration of CEA is 8×10^{-11} mol/L, while the concentrations of other interferents are 1×10^{-6} mol/L.

4. Conclusions

In summary, a new selective and sensitive colorimetric sensing system for CEA by merging the speediness and convenience of colorimetric assay with isothermal and exponential amplification of HRCAs technology has been developed. This homogeneous assay system not only eliminates the thermal cycling but also achieves improved assay characteristics (e.g., the wide linear response range, low detection limit and high specificity). It holds promising potential for broad applications in biodetection of diseases, biochemical study, environmental and in clinical applications

Acknowledgement

This project was partly financially supported by the National Basic Research Program of China (No.2010CB732403), and the Program for Changjiang Scholars and Innovative Research Team in University (No. IRT1116), the national Key Technologies R&D Program of China during the 12th five year plan period (2012BAD29B06, 2012BAK01B01) and Major Project of Fujian Provincial Science and Technology program (2011N5008).

Notes and references

^a Henan provincial people's hospital, Zhengzhou, Henan 450003, China

^b Department of Chemistry, Fuzhou University, Fuzhou, Fujian

350108, China. E-mail: summer328cn@163.com (B. Qiu);

shaojingwei@fzu.edu.cn (J.W. Shao);

1 S. R.Tang, P.Tong, H.Li, J.Tang and L. Zhang, *Biosens. Bioelectron.* **2013**, *42*, 608–611.

2 Z. S.Wu, H.Zhou, S. B.Zhang, G. L.Shen and R. Yu, *Anal. Chem.* **2010**, *82*, 2282–2289.

3 P. M.Lizardi, X. H.Huang, Z. G.Zhu, P.Bray-Ward, D. C.Thomas and D. C. Ward, *Nat. Genet* **1998**, *19*, 225–232.

4 D. Y.Zhang, W. D.Zhang, X. P.Li and Y.Konomi, *Gene* **2001**, *274*, 209–216.

5 Y. Q.Cheng, X.Zhang, Z.Li, X.Jiao, Y.Wang and Y.Zhang, *Angew. Chem., Int. Ed.* **2009**, *121*, 3318–3322.

6 A. P.Cao and C. Y.Zhang, *Anal. Chem.* **2012**, *84*, 6199–6205.

7 Y.Long, X. Zhou and D.Xing, *Biosens. Bioelectron.* **2011**, *26*, 2897–2904.

8 P. K.Jain, K. S.Lee, I. H. El-Sayed and M. A. El-Sayed, *J. Phys. Chem. B* **2006**, *110*, 7238–7248.

9 M. M.Alvarez, J. T.Khoury, T. G.Schaaff, M. N. Shafgullin, I.Vezmar, and R. L. Whetten, *J. Phys. Chem. B* **1997**, *101*, 3706–3712.

10 S. K.Ghosh, A.Pal, S.Kundu, S.Nath and T.Pal, *Chem. Phys. Lett.* **2004**, *395*, 366–372.

11 J.Zhang, L.Wang, D.Pan, S.Song, F. Y. C. Boey, H.Zhang and C. Fan, *Small* **2008**, *4*, 1196–1200.

12 R.Kanjanawarut and X.Su, *Anal. Chem.* **2009**, *81*, 6122–6129.

13 S. J.Chen, Y. F.Huang, C. C.Huang, K. H.Lee, Z. H. Lin and H. T.Chang, *Biosens. Bioelectron.* **2008**, *23*, 1749–1753.

14 F.Luo, L.Y.Zheng, S.S.Chen, Q. H. Cai, Z. Y.Lin, B.Qiu and G. N. Chen, *Chem. Commun.* **2012**, *48*, 6387–6389.

15 M.Szemes, P.Bonants, M. D.Weerd, J.Baner, U.Landegren and C. D.Schoen, *Nucleic Acids Res.* **2005**, *33*, e70.

16 P. R.Srinivas, S.Srivastava, S.Hanash and G. L.Wright, *Clin. Chem.* **2001**, *47*, 1901–1911.

17 S. K.Arya and S.Bhansali, *Chem. Rev.* **2011**, *111*, 6783–6809.

18 M.Ferrari, *Nat. Rev. Cancer* **2005**, *5*, 161–171.

19 M. K.Boehm, M. O. Mayans, J. D.Thornton, R. H. J.Begent, P. A.Keep and S. J.Perkins, *J. Mol. Biol.* **1996**, *259*, 718–736.

20 G. R. H. Tabar, C. L. Smith, *J. World Appl. Sci.* **2010**, *8*, 16.

21 Patent Application Publication, US 2010/0254901 A1, Oct. 7, 2010

22 K. C.Grabar, R. G.Freeman, M. B.Hommer and M. J.Natan, *Anal. Chem.* **1995**, *67*, 735–743.

23 T.Murakami, J.Sumakoka and M.Komiyama, *Nucleic Acids Res.* **2009**, *37*, e19.

24 J. Y.Hou, T. C.Liu, G. F.Lin, Z. X.Li, L. P.Zou, M. Li and Y. S. Wu, *Anal. Chim. Acta* **2012**, *734*, 93–98.

25 W. Dungchai, W.Siangproh, J. M. Lin, O.Chailapakul, S. Lin and X.Ying, *Anal. Bioanal. Chem.* **2007**, *387*, 1965–1971.

26 J.Pan and Q. Yang, *Anal. Bioanal. Chem.* **2007**, *388*, 279–286.